Journal of the Ceramic Society of Japan 113 [8] 519-524 (2005)

Paper

Structural Changes in $RSiO_{3/2}$–TiO_2 Hybrid Films with UV Irradiation and Their Photocatalytic Micropatterning

Teruyuki SASAKI,† Atsunori MATSUDA,* Kiyoharu TADANAGA and Masahiro TATSUMISAGO

Department of Applied Materials Science, Graduate School of Engineering, Osaka Prefecture University, 1-1, Gakuen-cho, Sakai-shi, Osaka 599-8531

**Department of Materials Science, Toyohashi University of Technology, 1-1, Hibarigaoka, Tempaku-cho, Toyohashi-shi, Aichi 441-8580*

紫外光照射による $RSiO_{3/2}$–TiO_2 系ハイブリッド膜の構造変化と光触媒作用によるマイクロパターニング

佐々木輝幸† · 松田厚範* · 忠永清治 · 辰巳砂昌弘

大阪府立大学大学院工学研究科機能物質科学分野，599-8531 大阪府堺市学園町 1-1

*豊橋技術科学大学物質工学系，441-8580 愛知県豊橋市天伯町雲雀ヶ丘 1-1

UV light irradiation induced structural changes of the cleavage of silicon–carbon bonds and elimination of organic groups in organosilsesquioxane-titania ($RSiO_{3/2}$–TiO_2, R = methyl, ethyl, phenyl and benzyl) hybrid films due to the photocatalytic effect of TiO_2 component. Phenyl and benzyl groups tended to remain in the films after the cleavage of Si–C bonds presumably due to their higher stability of aromatic rings and lager steric effect. The refractive index and dynamic hardness of all the hybrid films increased, and the thickness and contact angle for water decreased by the structural changes induced by the UV light irradiation. On the basis of these changes in film properties, micropatterning was successfully performed on the $RSiO_{3/2}$–TiO_2 hybrid films by UV light irradiation through a photomask. The micropatterns thus obtained should be applicable to a printing plate using the surface energy differences as well as a micro-optical component using the surface profiles and refractive index changes.

［Received February 21, 2005; Accepted June 16, 2005］

Key-words : *Micropattern, Hybrid, UV irradiation, Organosilsesquioxane, Titania, Micro-optics, Printing*

1. Introduction

Inorganic–organic hybrid materials have attracted significant attention in recent years.[1),2)] The sol–gel process using metal alkoxides as starting materials has a great potential for the preparation of variously shaped inorganic–organic hybrid materials such as films, microparticles and membranes. The thickness of inorganic, oxide films prepared by the sol–gel process is generally limited to less than 1 μm due to cracking, whereas thickness more than a few μm is attainable without cracking by incorporating organic components in the films.[3),4)] Furthermore, we can provide the newly designed optical, mechanical and thermal properties such as refractive index, flexibility and thermoplasticity, which are not achieved by only inorganic components, by the selection of organic components.[5)-8)] Organosilsesquioxane ($RSiO_{3/2}$), in which organic functional groups R have covalently bonded to siloxane structure, is a promising inorganic-organic hybrid material in the molecular level. The physical and chemical properties of $RSiO_{3/2}$ can be controlled by varying the concentration and the type of R in siloxane network.[9)-13)]

On the other hand, TiO_2-containing inorganic–organic materials have been extensively studied for their application to optical coatings and micro-optic devices because of their high refractive indices as well as good thermal and chemical durability.[14)-18)] With respect to the use of photocatalytic activity of TiO_2, Tada et al. reported that photocatalytic decomposition of the organic groups in chemisorbed methylsiloxane layer on an anatase TiO_2 lower layer during UV light irradiation.[19),20)] We also reported the fabrication of superhydrophobic-superhydrophillic micropatterns based on a fluoroalkylsilane/TiO_2/flowerlike alumina multilayer on the substrate and UV irradiation on the selected area for the multilayer through a photomask. Only the UV irradiated areas become hydrophilic because of the decomposition of fluoroalkyl groups in the upper layer by a photocatalytic activity of the TiO_2 lower layer, while the unirradiated areas remain hydrophobic.[21)] However, the photocatalytic decomposition of organic groups in the thick $RSiO_{3/2}$ films is difficult by the above two processes using the TiO_2 layers.

Recently, we have proposed a new micropatterning process, which has a great potential for designing the micro-optics components and micro-printing plates, using UV photolithography for ethylsilsesquioxane-titania ($EtSiO_{3/2}$–TiO_2) hybrid film.[22)] This process is based on the irreversible structural changes in the films caused by the cleavage of Si–C bonds by the photocatalytic activity of the TiO_2 component during UV irradiation. In addition, these structural changes by the UV irradiation induce the changes of film properties, such as the refractive index, the contact angle for water and the hardness. Such micropattering process is becoming more important in the fabrication of refractive index-controlled micro-optic devices like gratings, waveguides, and optical circuits.[23)-25)] For further progress in the photocatalytic micropatterning for the hybrid films, detailed studies on the effect of organic groups on the changes in the physical and chemical properties as well as in the structure of the films are essential. This paper reports the structural changes in the several kinds of $RSiO_{3/2}$–TiO_2 (R = Me(CH_3–), Et(CH_3CH_2–), Ph(C_6H_5–), Bn(C_6H_5–

† Present address: Technical Research Laboratory, Kansai Research Center, Nippon Sheet Glass Co., Ltd., 1, Kaidoshita, Konoike, Itami-shi, Hyogo 664-8520
現在：日本板硝子(株)技術研究所関西研究センター，664-8520 兵庫県伊丹市鴻池字街道下 1

CH_2–)) hybrid films with UV irradiation. The difference of the effects of organic group R on the film properties has been discussed. The micropatterning of the hybrid films based on the photocatalytic effect of the TiO_2 component has been also described.

2. Experimental

2.1 Preparation of hybrid films

Preparation procedure of $80RSiO_{3/2}\cdot 20TiO_2$ (in mol%, R = Me, Ph and Bn) hybrid films is essentially the same as that of $80EtSiO_{3/2}\cdot 20TiO_2$ film described in the preceding paper.[22] Several kinds of organotriethoxysilanes ($RSi(OEt)_3$ (R = Me, Et, Ph and Bn), Shin-Etsu Chemical Industries) and titanium tetra-*n*-butoxide ($Ti(O\text{-}n\text{-}Bu)_4$, Wako Pure Chemical Industries) were used as the starting materials. $RSi(OEt)_3$ in ethanol (EtOH) was hydrolyzed with diluted hydrochloric acid of 0.1 mass% HCl at room temperature for 30 min. The molar ratio of $RSi(OEt)_3$:H_2O:EtOH was 0.8:4:1. $Ti(O\text{-}n\text{-}Bu)_4$ in EtOH was chemically modified with ethylacetoacetate (EAcAc, Kishida Chemical Co., Ltd.) by stirring the solution at room temperature for 1 h. The molar ratio of $Ti(O\text{-}n\text{-}Bu)_4$:EtOH:EAcAc was 1:20:1. The modified $Ti(O\text{-}n\text{-}Bu)_4$ solution was added to the hydrolyzed $RSi(OEt)_3$ solution and stirred continuously for 30 min. The clear sols obtained were filtered using a 0.45-μm filter (GL Chromato Disk, Kurabo, Ind., Ltd.) and served as coating solutions.

The coating was carried out by dipping-withdrawing of a substrate with a speed of 0.45–1.11 mm/s in an ambient atmosphere. Silica glass plates, soda–lime–silica glass plates, and silicon wafers were used as the substrates for coating. The substrates coated with films were dried at room temperature for 40 min and then heat-treated at 150°C for 1 h.

UV light irradiation on the films was carried out using an ultra-high-pressure mercury lamp (UIS-25102 250 W, Ushio Inc.). The intensity of the UV light was measured using an illumination photometer (UIT-150-A, Ushio Inc.) with detectors S365 and S254. The intensities of the light irradiated were 82 mW/cm^2 in a range of 310–390 nm and 22 mW/cm^2 in a range of 220–310 nm. The maximum temperature of the films coated on glass substrates during UV light irradiation for 240 min under the conditions above was lower than 50°C, which was monitored using a thermocouple.

2.2 Characterization of hybrid films

Fourier transformed infrared (FT-IR) absorption spectra of the films coated on silicon substrates were measured in a transmission mode using an FT-IR spectrophotometer (FT-IR1650, PerkinElmer). Ultraviolet–visible (UV-Vis) transmission spectra of the film, which was coated on the one side of silica glass or soda–lime–silica glass substrates, were obtained using a UV-Vis spectrophotometer (V-560, JASCO). The refractive index and thickness of the film were calculated from wavy patterns in the UV-Vis transmission spectra due to the interference between the film and the substrate.[26] In the calculation, refractive indices of 1.46 and 1.52 were adopted for silica glass and soda–lime–silica–glass, respectively. Changes in microhardness and contact angle for water of the films with UV irradiation were measured using a dynamic ultra microhardness tester (DUH-W201, Shimadzu Corp.) and a contact angle meter (CA-C, Kyowa Surface Science), respectively. X-ray diffraction (XRD) patterns of the films before and after UV irradiation were measured using an X-ray diffractometer (M18XHF22-SRA, Mac Science). The texture of the films before and after UV light irradiation was observed using a field-emission-type scanning electron microscope (FE-SEM, S-4500, Hitachi Ltd.) and a field-emission-type transmission electron microscope (FE-TEM, HF-2000, Hitachi Ltd.).

2.3 Micropatterning on hybrid films with UV irradiation

The micropatterning process on the hybrid films with UV irradiation was essentially the same as in our previous paper.[22] UV light was irradiated against the film coated on the substrate through a photomask. Metal meshes with 30-μm squares through holes in 60-μm pitch were mainly used as a phtomask. The surface of the patterned film with UV light irradiation was observed on an optical microscope (Model BX50, Olympus Co.). The three-dimensional shapes of the micropatterns formed in the films were evaluated using an atomic force microscopy (AFM, Nanopics, Seiko Instruments Inc.) and a three-dimensional surface profilometer (TDA-22, Kosaka Laboratory Ltd.).

3. Results and discussion

3.1 Comparison of structural changes in hybrid films with UV irradiation

FT-IR absorption spectra of $80RSiO_{3/2}\cdot 20TiO_2$ hybrid films coated on silicon substrates and irradiated with UV light for 240 min have been measured. In the FT-IR spectra of all the $RSiO_{3/2}$–TiO_2 hybrid films, a broad and intense absorption band at around 1100 cm^{-1} assigned to Si–O–Si bond and a band at around 930 cm^{-1} assigned to Si–O–Ti bonds in which titanium ions were incorporated in the four-coordinated state[27),28)] were observed. Absorption bands due to Si–C and C–H bonds were, respectively, observed at around 1300 and 3000 cm^{-1} for $MeSiO_{3/2}$– and $EtSiO_{3/2}$–TiO_2 hybrid films, while those were seen at around 1200 and 3100 cm^{-1} for $PhSiO_{3/2}$– and $BnSiO_{3/2}$–TiO_2 hybrid films. The intensities of absorption peaks due to Si–C bonds and C–H bonds in the spectra of all the films gradually decreased with UV irradiation accompanied by a decrease in the intensity of the absorption band due to Si–O–Ti bonds. In addition, the intensity of a broad band at around 3400 cm^{-1} due to OH bonds increased concomitantly by these spectral changes during UV irradiation. These results indicate that organic groups in all the $RSiO_{3/2}$–TiO_2 hybrid film were eliminated after the cleavage of Si–C bonds and Si–O–Ti bonds were dissociated to form –OH and/or Si–O–Si bonds. No decrease in Si–C bonds was observed for the films without incorporation of TiO_2 during UV irradiation. Therefore, these structural changes with the irradiation are caused by the photocatalytic effect of the TiO_2 component in the hybrid. Consequently, structural changes in these $RSiO_{3/2}$–TiO_2 hybrid films with UV irradiation proceed through the cleavage of Si–C and Si–O–Ti bonds and the formation of –OH bonds such as Si–OH and Ti–OH groups. With respect to the effect of EAcAc, the thermal decomposition of Ti-EAcAc complex and disappearance of EAcAc in the hybrid films at 80°C were confirmed from the IR absorption spectra. Therefore, EAcAc used for chemical modification of $Ti(O\text{-}nBu)_4$ has little influence on the above structural changes of the $RSiO_{3/2}$–TiO_2 hybrid films by UV irradiation because all the films were heat-treated at 150°C before the irradiation.

The changes in the normalized intensities of the absorption peaks assigned to (a) Si–C and (b) Si–O–Ti bonds in the FT-IR spectra of $80RSiO_{3/2}\cdot 20TiO_2$ hybrid films with UV irradiation are shown in **Fig. 1.** The intensities of the absorption peaks were normalized with those of the film before the irradiation. The intensity of the peaks assigned to Si–C bonds decreases with UV irradiation in 240 min to become 0.65 (R = Me), 0.45 (R = Et), 0.55 (R = Ph) and 0.45 (R = Bn) of that of the film before the irradiation, indicating that Si–C bonds

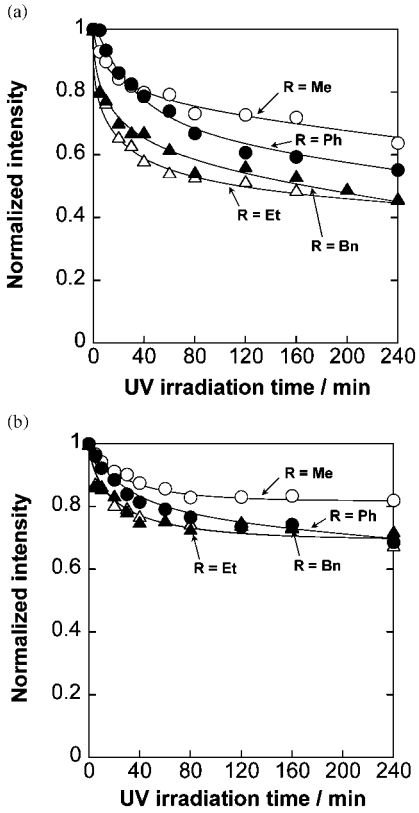

Fig. 1. Changes in the normalized intensities of the absorption peaks assigned to (a) Si–C and (b) Si–O–Ti bonds in the FT-IR spectra of $80RSiO_{3/2}\cdot 20TiO_2$ (R = Me, Et, Ph and Bn) hybrid films with UV irradiation. The intensities of the absorption peaks were normalized with those of the film before the irradiation.

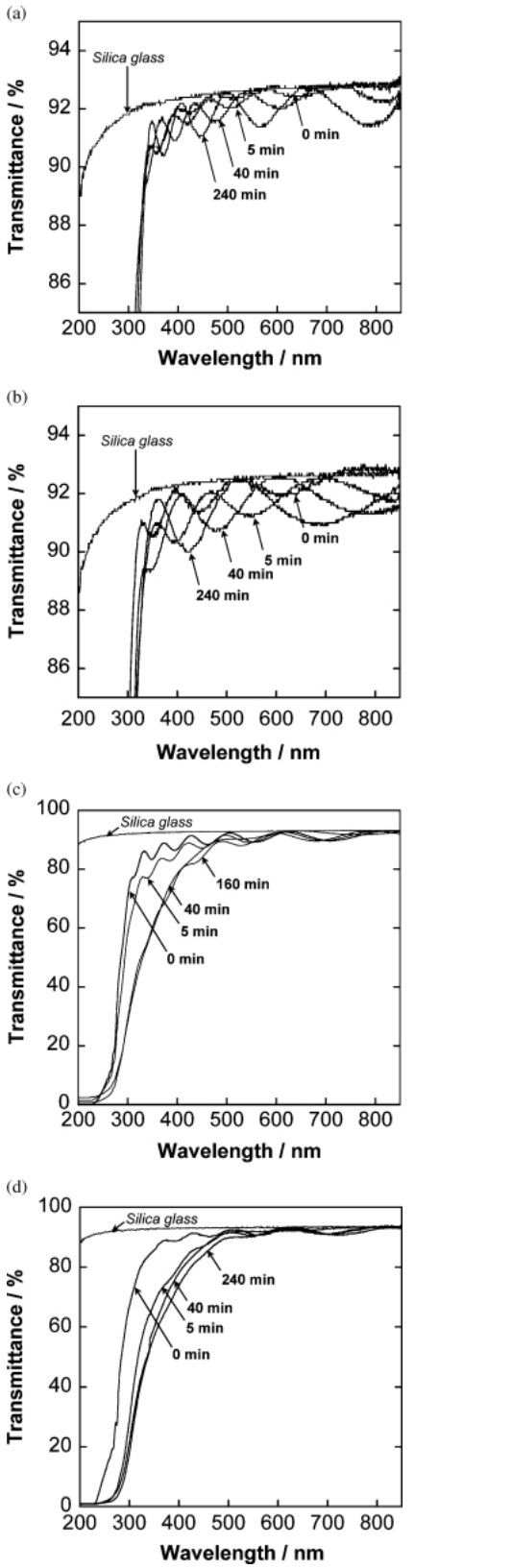

Fig. 2. Optical transmission spectra of the $80RSiO_{3/2}\cdot 20TiO_2$ hybrid films coated on one side of the silica glass substrates which were heat-treated at 150°C for 1 h and irradiated with UV light for various periods of time. (a), (b), (c) and (d) are for the $80RSiO_{3/2}\cdot 20TiO_2$ of R = Me, Et, Ph and Bn, respectively.

in the films are cleaved by 35, 55, 45 and 55%, respectively, (Fig. 1(a)). The decrease in the intensity of the peak due to Si–C bonds with UV irradiation was accompanied by the decrease of a peak assigned to C–H bonds at around 3000 cm^{-1}, indicating the cleaved organic groups probably left the film after UV irradiation. Si–C bonds in $MeSiO_{3/2}$ were the most stable against UV irradiation among the $RSiO_{3/2}$ examined, whereas methyl groups were desorbed from the film just after the cleavage of Si–C bonds. On the other hand, phenyl and benzyl groups in the hybrid films were found to remain in the films presumably due to their higher stability of aromatic rings and lager steric effect after the cleavage of Si–C bonds.

The intensity of the peak assigned to Si–O–Ti bonds decreases with UV irradiation in 240 min to become about 0.8 (R = Me), 0.7 (R = Et), 0.7 (R = Ph) and 0.7 (R = Bn) of those in the films before the irradiation, indicating that Si–O–Ti bonds in the films are dissociated with UV irradiation (Fig. 2(b)). The decrease in the amounts of Si–C bonds shown in **Fig. 2**(a) corresponds to that in the amounts of Si–O–Ti bonds shown in Fig. 2(b). This suggests that dissociation of Si–O–Ti bonds is closely related to the photocatalytic cleavage of Si–C bonds.

XRD measurements showed that all the hybrid films before and after UV irradiation were amorphous. In addition, TEM observation of the films irradiated with UV light revealed that no crystalline phases and no inhomogenieties were present in the films. TiO_2 component present in $RSiO_{3/2}$–TiO_2 hybrids absorbs UV light and the excited electrons probably cleave the Si–C bonds. The cleavage of Si–C bonds should induce the dissociation of Si–O–Ti bonds in the hybrid films. The

cleavage of Si–C bonds with UV irradiation occurred owing not to titania crystallites but to amorphous titania component in which titanium ions were incorporated in a four-coordinated state in silsesquioxane as shown by the IR absorption spectra.

3.2 Comparison of physical and chemical changes in hybrid films with UV irradiation

Optical transmission spectra of the $80RSiO_{3/2}\cdot 20TiO_2$ hybrid films coated on one side of the silica glass substrates which were heat-treated at 150°C for 1 h and irradiated with UV light for various periods of time are shown in Fig. 2: (a), (b), (c) and (d) are for the $80RSiO_{3/2}\cdot 20TiO_2$ of R = Me, Et, Ph and Bn, respectively. In the spectra of $MeSiO_{3/2}$– and $EtSiO_{3/2}$–TiO_2 films (Figs. 2 (a) and (b)), the maxima of wavy transmission spectra are as high as that of the substrate without coating, so that the films are highly transparent even after the UV irradiation. The minima of transmission wavy patterns of $MeSiO_{3/2}$– and $EtSiO_{3/2}$–TiO_2 films decrease and shift to shorter wavelength with UV irradiation, indicating that the refractive index of the film increases and the film thickness decreases during irradiation. On the other hand, $PhSiO_{3/2}$– and $BnSiO_{3/2}$–TiO_2 films (Figs. 2(c) and (d)) without UV irradiation are highly transparent before UV irradiation, while the transmittance at shorter wavelength decreases and the absorption edge shifts to longer wavelength with the irradiation. These optical changes in $PhSiO_{3/2}$– and $BnSiO_{3/2}$–TiO_2 films with UV irradiation are not observed in the $MeSiO_{3/2}$– and $EtSiO_{3/2}$–TiO_2 (Figs. 2(a) and (b)). This may be ascribed to the higher stability and larger steric effect of aromatic rings in phenyl and benzyl groups than alkyls such as methyl and ethyl groups in the films after the cleavage of Si–C bonds. Neither crystalline phase nor inhomogeneity was observed on TEM in the hybrid films with aromatic rings after UV irradiation. Thus the remaining, degraded aromatic rings should cause the UV-Vis absorption in the region with a longer wavelength than 250 nm.

Figure 3 shows changes in (a) refractive index and (b) thickness of $80RSiO_{3/2}\cdot 20TiO_2$ (R = Me, Et, Ph and Bn) hybrid films during UV irradiation. The irradiation time was within 40 min because of the slight coloration of $PhSiO_{3/2}$– and $BnSiO_{3/2}$–TiO_2 films. The refractive index and thickness were calculated from the minima and wavelength at around 600 nm in the optical transmission spectra. It is seen that the refractive index of the hybrid film can be controlled by the selection of the organic group and the indices of all the films increase with the UV irradiation. $MeSiO_{3/2}$–TiO_2 film has the lowest refractive index, which increases from 1.48 to 1.50 by UV irradiation for 40 min. Those of $EtSiO_{3/2}$–, $PhSiO_{3/2}$– and $BnSiO_{3/2}$–TiO_2 films increase from 1.52 to 1.55, from 1.58 to 1.61, and from 1.55 to 1.57 with the irradiation, respectively (Fig. 3(a)). The thickness of each film decreases with UV irradiation, which corresponds to the increase in the refractive index of the film (Fig. 3(b)). These phenomena indicate that the films are densified with UV irradiation. The thickness of $MeSiO_{3/2}$–TiO_2 film decreases from 0.79 to 0.73 μm by about 8% after a UV light irradiation for 40 min followed by the increase in refractive index from 1.48 to 1.50. The values of shrinkage in $PhSiO_{3/2}$– and $BnSiO_{3/2}$–TiO_2 films are 11 and 3%, respectively, whereas that of $EtSiO_{3/2}$–TiO_2 is 25%. Although the increases in refractive index of the hybrid films are almost same (0.02–0.03), the decrease in thickness of $EtSiO_{3/2}$–TiO_2 film is larger than those of the other $RSiO_{3/2}$–TiO_2 films. The larger decrease in thickness of the $EtSiO_{3/2}$–TiO_2 film is caused by the larger amount of cleaved Si–C bonds and by more readily eliminated alkyl groups as described in the preceding Section 3.1.

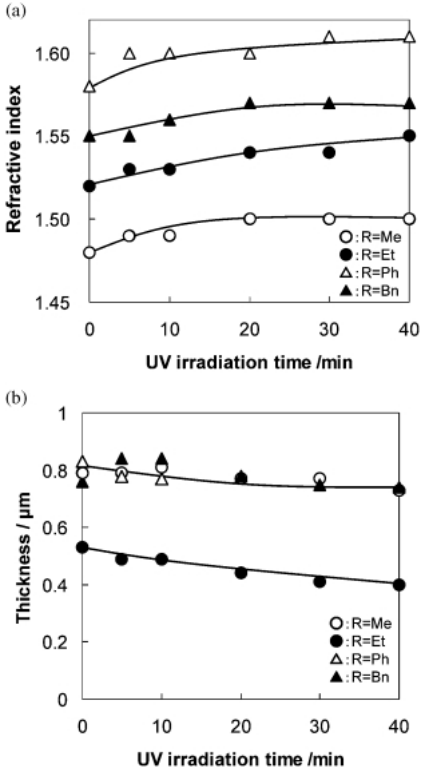

Fig. 3. Changes in (a) refractive index and (b) thickness of $80RSiO_{3/2}\cdot 20TiO_2$ (R = Me, Et, Ph and Bn) hybrid films during UV irradiation.

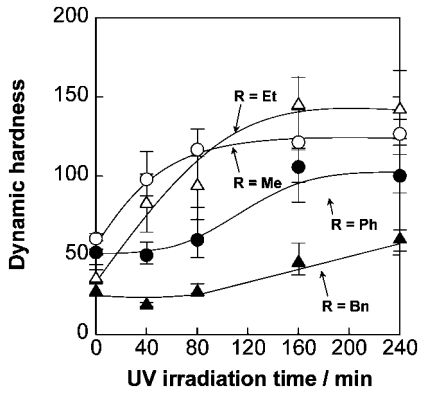

Fig. 4. Changes in dynamic hardness of the $80RSiO_{3/2}\cdot 20TiO_2$ (R = Me, Et, Ph and Bn) hybrid films with UV irradiation. Error bars show the range between the maximum and minimum values of the repeated measurements.

Figure 4 shows dynamic hardness change of the $80RSiO_{3/2}\cdot 20TiO_2$ hybrid films with UV irradiation. Error bars show the range between the maximum and minimum values of the repeated measurements. The hardness of all the films increases with UV irradiation time, which is attributed to the densification of the films. $MeSiO_{3/2}$– and $EtSiO_{3/2}$–TiO_2 films show higher hardness and steeper increase in hardness than $PhSiO_{3/2}$– and $BnSiO_{3/2}$–TiO_2 during UV irradiation. In the $PhSiO_{3/2}$– and $BnSiO_{3/2}$–TiO_2 films, the hardness gradually increases. This probably reflects the presence of phenyl and benzyl groups in the hybrid films after the cleavage of Si–C bonds

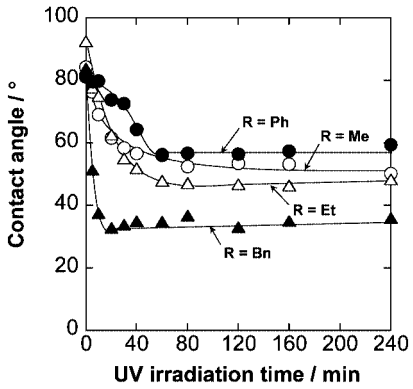

Fig. 5. Changes in the contact angle for water of the $80RSiO_{3/2}\cdot 20TiO_2$ (R = Me, Et, Ph and Bn) hybrid films with UV light irradiation.

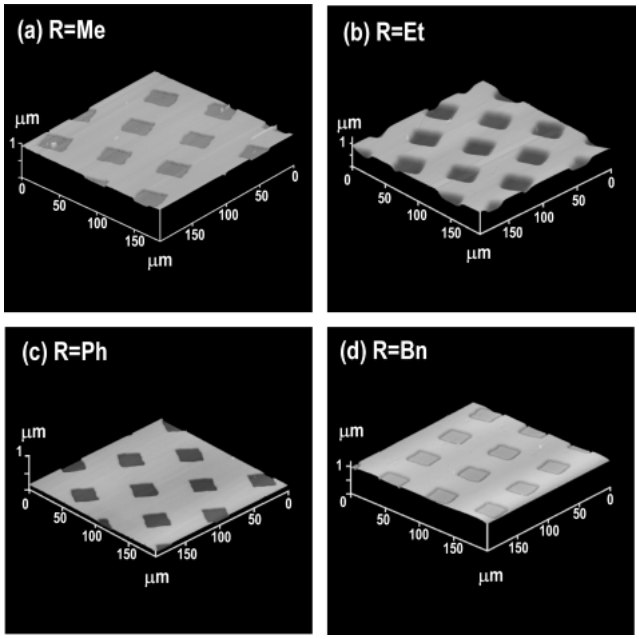

Fig. 6. AFM images of the surface of the $80RSiO_{3/2}\cdot 20TiO_2$ hybrid films after UV irradiation for 40 min through a photomask. (a), (b), (c) and (d) are for the $80RSiO_{3/2}\cdot 20TiO_2$ of R = Me, Et, Ph and Bn, respectively.

with UV irradiation. The hardness of polystyrene substrates was *ca.* 20 under the same conditions. The $RSiO_{3/2}$–TiO_2 hybrid films can be formed not only on glass and metals but also on plastics, so that the films are promising as protective coatings and hard coatings for plastic substrates like goggles.

Figure 5 shows contact angle for water of the $80RSiO_{3/2}\cdot 20TiO_2$ hybrid films irradiated with UV light. Before UV irradiation, all the hybrid films are hydrophobic, *i.e.*, contact angles for water are higher than 80°, due to the corresponding organic group. The contact angle of the films decreases with UV irradiation, which is attributed to the decrease in the amount of organic groups at the surface of the films due to photocatalytic effect of TiO_2. In $BnSiO_{3/2}$–TiO_2 hybrid film, the contact angle steeply decreases from 82° to 34° in 40 min, so that hydrophobic-hydrophilic patterns with a relatively large difference in the contact angles can be designed in this system. The tendency of the decrease in the contact angle for water of the film with UV irradiation can be attributed to the state of the organic groups especially at the surface of the films.

3.3 Photocatalytic micropatterning of hybrid films

UV light was irradiated on the $80RSiO_{3/2}\cdot 20TiO_2$ hybrid films coated on the substrate using a metal mesh with 30-μm squares through holes in 60-μm pitch as a photomask. AFM images of the surface of the $80RSiO_{3/2}\cdot 20TiO_2$ hybrid films after UV irradiation for 40 min are shown in **Figs. 6** (a), (b), (c) and (d) are for the $80RSiO_{3/2}\cdot 20TiO_2$ of R = Me, Et, Ph and Bn, respectively. Arrayed dark squares are concave areas, which correspond to the through holes of the metal mesh used as a photomask. The depth of the concave areas on the $MeSiO_{3/2}$–, $EtSiO_{3/2}$–, $PhSiO_{3/2}$– and $BnSiO_{3/2}$–TiO_2 hybrid films was 0.09, 0.11, 0.05 and 0.03 μm, which was 11, 18, 7 and 3% of the initial thickness of the films before UV irradiation. The shrinkage in the areas on which UV light was irradiated through the photomask is fairly close to that of the film after UV light irradiation without a photomask shown in Fig. 3(b). Thus, the influence of the neighboring unirradiated areas on the shrinkage of the film during UV irradiation should be relatively small. Micropatterns and microdots based on the refractive index change can be also formed in the films using this process. For example, $BnSiO_{3/2}$–TiO_2 film shows a larger refractive index change with a smaller shrinkage after UV irradiation. This suggests that $BnSiO_{3/2}$–TiO_2 film has a great potential to fabricate flat-type optical components. In the $EtSiO_{3/2}$–TiO_2 hybrid film a larger shrinkage is obtained with UV irradiation, while the refractive index change is almost the same as $BnSiO_{3/2}$–TiO_2. That is, the geometrical patterns with a high aspect ratio for optical components can be formed on the $EtSiO_{3/2}$–TiO_2 film with UV irradiation. Moreover, the changes in the optical properties, surface profiles, and chemical and physical properties of the $RSiO_{3/2}$–TiO_2 hybrid films with UV light irradiation can be controlled by not only varying the organic groups R but also UV exposure conditions.

This micropatterning process is based on the irreversible structural changes in the hybrid films caused by the cleavage of Si–C bonds during UV irradiation. Therefore, the shape of the resultant patterns is quite stable upon storage for a long period of time. In addition, UV light irradiated areas show higher hardness and lower contact angle for water than the UV light unirradiated areas as shown in Figs. 4 and 5. One of the promising applications of such hydrophobic-hydrophilic micropatterns is a printing plate, which holds ink on the hydrophilic areas and imprints it on another surface. In Fig. 5, changes in the contact angle for water with UV irradiation is largest in $BnSiO_{3/2}$–TiO_2 film with UV irradiation, which proves the significant difference in the wettability between the UV irradiated and unirradiated areas. Micropatterned $BnSiO_{3/2}$–TiO_2 film with UV light irradiation is, thus, promising for the microprinting process. The thickness of $RSiO_{3/2}$–TiO_2 hybrid films can be increased up to about 1 μm, so the abrasion resistance in repeated printings is expected for the patterned films.

4. Conclusions

UV irradiation on $RSiO_{3/2}$–TiO_2 (R = Me, Et, Ph, Bn) hybrid films caused the cleavage of the Si–C bonds and the dissociation of Si–O–Ti bonds to form –OH groups and/or Si–O–Si bonds due to the photocatalytic effects of TiO_2 component. Alkyl groups in $MeSiO_{3/2}$– and $EtSiO_{3/2}$–TiO_2 films were eliminated just after the cleavage of Si–C bonds with UV irradiation, so that the refractive index was increased accom-

panied by the large decrease in the film thickness. On the other hand, aromatic rings in $PhSiO_{3/2}$– and $BnSiO_{3/2}$–TiO_2 films were relatively stable for the UV light and tended to remain in the film after the cleavage of Si–C bonds. The increase in dynamic hardness of $MeSiO_{3/2}$– and $EtSiO_{3/2}$–TiO_2 films was larger than that of $PhSiO_{3/2}$– and $BnSiO_{3/2}$–TiO_2 films because of their larger shrinkage followed by the elimination of the alkyl groups induced by the UV irradiation.

Micropatterning on the $RSiO_{3/2}$–TiO_2 hybrid films coated on the substrate was successfully carried out by UV irradiation through a photomask. The changes in the optical properties, surface profiles and chemical and mechanical properties of the $RSiO_{3/2}$–TiO_2 hybrid films with UV irradiation can be controlled by varying the organic group *R* in the hybrid films and UV exposure conditions. This micropatterning process has a great potential to fabricate micro-optic and photonic components such as gratings, waveguides and optical circuits. In addition, micropatterned hydrophobic-hydrophilic surface thus obtained can be used as a microprinting plate.

Acknowledgment The authors thank Dr. Toshihiro Kogure of The University of Tokyo for the TEM observation and valuable discussion. This work was partly supported by the Japan Society for the Promotion of Science (JSPS) (Grant-in-Aid for Scientific Research (B), No. 16360327). AM acknowledges Izumi Science and Technology Foundation and Hosokawa Powder Technology Foundation for their financial support.

References

1) Roy, D. A. and Shea, K. J., *Chem. Rev.*, Vol. 95, pp. 1431–1442 (1995).
2) Sanchez, C., Soler-Illia, G. J. de A. A., Ribot, F., Lalot, T., Mayer, C. R. and Cabuil, V., *Chem. Mater.*, Vol. 13, pp. 3061–3083 (2001).
3) Innocenzi, P., Abdirashid, M. O. and Guglielmi, M., *J. Sol–Gel. Sci. Technol.*, Vol. 3, pp. 47–55 (1994).
4) Kozuka, H., *J. Ceram. Soc. Japan*, Vol. 111, pp. 624–632 (2003).
5) Schmidt, H., *J. Non-Cryst. Solids*, Vol. 73, pp. 681–691 (1985).
6) Boulton, J. M., Thompson, J., Fox, H. H., Gorodisher, I., Teowee, G., Calvert, P. D. and Uhlmann, D. R. "Better Ceramics Through Chemistry 4," Ed. by Zellinski, B. J. J., Brinker, C. J., Clark, D. E. and Ulrich, D. R., Material Research Society (1990) pp. 987–987.
7) Saravanamuttu, K., Du, X. M., Najafi, M. P. and Andrews, S. I., *Can. J. Chem.*, Vol. 76, pp. 1717–1729 (1998).
8) Saegusa, T. and Chujo, Y., *J. Macromole. Sci. A, Chem.*, Vol. 27, pp. 1603–1612 (1990).
9) Baney, R. H., Itoh, M., Sakakibara, A. and Suzuki, T., *Chem. Rev.*, Vol. 95, pp. 1409–1430 (1995).
10) Murakami, M., Izumi, K., Deguchi, T., Morita, A., Tohge, N. and Minami, T., *J. Ceram. Soc. Japan*, Vol, 97, pp. 91–93 (1989).
11) Mackenzie, J. D., Huang, Q. and Iwamoto, T., *J. Sol–Gel. Sci. Technol.*, Vol. 7, pp. 151–161 (1996).
12) Matsuda, A., Matsuno, Y., Tatsumisago, M. and Minami, T., *J. Am. Ceram. Soc.*, Vol. 81, pp. 2849–2852 (1998).
13) Matsuda, A., Sasaki, T., Hasegawa, K., Tatsumisago, M. and Minami, T., *J. Ceram. Soc. Japan*, Vol. 108, pp. 830–835 (2000).
14) Sorek, Y. and Reisfeld, R., *Appl. Phys. Lett.*, Vol. 63, pp. 3256–3258 (1993).
15) Que, W., Sun, Z., Zhou, Y., Lam, Y. M., Chan, Y. C. and Kam, C. H., *Thin Solid Films*, Vol. 358, pp. 16–21 (2000).
16) Yamada, N., Yoshinaga, I. and Katayama, S., *J. Appl. Phys.*, Vol. 85, pp. 2423–2427 (1999).
17) Yamada, N., Yoshinaga, I. and Katayama, S., *J. Sol–Gel. Sci. Technol.*, Vol. 17, pp. 123–130 (2000).
18) Que, W., Zhou, Y., Lam, Y. L., Chan, Y. C., Cheng, S. D., Sun, Z. and Kam, C. H., *J. Sol–Gel. Sci. Technol.*, Vol. 18, pp. 77–83 (2000).
19) Tada, H., *Langmuir*, Vol. 12, pp. 966–971 (1996).
20) Tada, H. and Tanaka, M., *Langmuir*, Vol. 13, pp. 360–364 (1997).
21) Tadanaga, K., Morinaga, J., Matsuda, A. and Minami, T., *Chem. Mater.*, Vol. 12, pp. 590–592 (2000).
22) Matsuda, A., Sasaki, T., Tadanaga, K., Tatsumisago, M. and Minami, T., *Chem. Mater.*, Vol. 14, pp. 2693–2700 (2002).
23) Xia, Y., Rogers, J. A., Paul, K. E. and Whitesides, G. M., *Chem. Rev.*, Vol. 99, pp. 1823–1848 (1999).
24) Eldada, L., *Opt. Eng.*, Vol. 40, pp. 1165–1178 (2001).
25) Schueller, O. J. A., Whitesides, G. M., Rogers, J. A., Meier, M. and Dodabalapur, A., *Appl. Opt.*, Vol. 38, pp. 5799–5820 (1999).
26) Yoldas, B. E., *Appl. Opt.*, Vol. 19, pp. 1425–1427 (1980).
27) Mukherjee, S. P., *J. Non-Cryst. Solids*, Vol. 42, pp. 477–488 (1980).
28) Morikawa, H., Osuka, T., Marumo, F., Yasumori, A. and Yamane, M., J. *Non-Cryst. Solids*, Vol. 82, pp. 97–102 (1986).